however, revealed multiple plaque rupture sites with thrombus formation distal to the site of plaque rupture (Fig. 1E).

On the other hand, cerebral infarction may also be associated with intact fibrous caps wherein only plaque fissure or erosion may constitute the substrate for thrombus formation (Figs. 1F and 1G). An 83-year-old man presented with sudden hemiplegia while he had his breakfast. On the day after the onset, angiography revealed an ipsilateral ischemic lesion with 80% stenosis of the right internal carotid artery. We performed OCT to characterize the tissue components of the culprit lesion. OCT revealed a plaque fissure with thrombus formation distal to the site of plaque fissure (Fig. 1F). Thrombus may also occur with an intact cap, which has been described in coronary arteries as plaque erosion (1). A 72-year-old man presented with stuttering hemiplegia. Fifteen days after onset, angiography revealed an ipsilateral ischemic lesion with 80% stenosis of the right internal carotid artery. The OCT revealed an intact fibrous cap with a double-lumen structure distal to the site of plaque erosion (Fig. 1G). Although only a few examples of ICA imaging are available in the literature, we expect that larger experience would help better the understanding of carotid plaques and allow more effective interventions in cerebral infarction.

Masanori Kawasaki, MD, PhD,* Shinichi Yoshimura, MD, PhD, Kiyofumi Yamada, MD, Arihiro Hattori, MD, Yoshiyuki Ishihara, MD, Kazuhiko Nishigaki, MD, PhD, Genzou Takemura, MD, PhD, Toru Iwama, MD, PhD, Shinya Minatoguchi, MD, PhD

*Department of Cardiology, Gifu University Graduate School of Medicine, 1-1 Yanagido, Gifu 501-1194, Japan. *E-mail: masanori@ya2.so-net.ne.jp*

http://dx.doi.org/10.1016/j.jcmg.2013.09.001

REFERENCES

1. Prati F, Uemura S, Souteyrand G, et al. OCT-based diagnosis and management of STEMI associated with intact fibrous cap. J Am Coll Cardiol Img 2013;6:283–7.
2. Ozaki Y, Okumura M, Ismail TF, et al. Coronary CT angiographic characteristics of culprit lesions in acute coronary syndromes not related to plaque rupture as defined by optical coherence tomography and angioscopy. Eur Heart J 2011;32:2814–23.
3. Yoshimura S, Kawasaki M, Hattori A, et al. Demonstration of intraluminal thrombus in the carotid artery by optical coherence tomography: technical case report. Neurosurgery 2010;67(3 Suppl Operative):onsE305, discussion onsE305.
4. Yadav JS, Wholey MH, Kuntz RE, et al., Stenting and Angioplasty With Protection in Patients at High Risk for Endarterectomy Investigators. Protected carotid-artery stenting versus endarterectomy in high-risk patients. N Engl J Med 2004;351:1493–501.
5. Schnaudigel S, Gröschel K, Pilgram SM, Kastrup A. New brain lesions after carotid stenting versus carotid endarterectomy: a systematic review of the literature. Stroke 2008;39:1911–9.

Myocardial Mechanics in Noncontiguous HCM

Marked phenotypic heterogeneity is typical of hypertrophic cardiomyopathy (HCM) with mostly localized and contiguous left ventricular hypertrophy. Rarely, noncontiguous but focal left ventricular hypertrophy is seen (1). A more comprehensive assessment of HCM, including segmental distribution of hypertrophy resulting in diverse patterns of HCM, has been described using cardiac magnetic resonance (CMR), and centerline chord method on CMR has been used to identify hypertrophied left ventricular segments that may otherwise go unidentified on conventional 2-dimensional echocardiography (2). A recent 3-dimensional CMR analysis showed that the majority of patients with asymmetrical septal HCM had a spiral pattern of hypertrophy, with extension toward complete concentric apical involvement seen in 10% of these patients (3,4). This finding suggests that asymmetric septal and apical HCM are not completely separate phenotypes. The continuum of disease involvement from base to apex can be underestimated in cross-sectional imaging, especially on a conventional 2-dimensional echocardiogram. However, the role of speckle tracking echocardiography in identification of such a continuum and in understanding the mechanics of myocardial dysfunction, especially in patients with noncontiguous HCM, is unclear.

We describe 5 cases of the noncontiguous left ventricular hypertrophy phenotype of HCM. All of these patients had localized hypertrophy involving the basal subaortic septal segment as well as circumferential hypertrophy of noncontiguous apical segments, with normal thickness (apparent sparing) of the intervening midventricular segments on conventional 2-dimensional echocardiography and CMR. However, speckle tracking–derived myocardial mechanics confirmed reduced longitudinal systolic strain not only of the hypertrophied segments of the apex and basal septum but also revealed abnormally reduced strain of the nonhypertrophied intervening midventricular segments (Fig. 1A). For comparison, we also describe patients with isolated basal septal hypertrophy, basal and midseptal hypertrophy, and apical hypertrophy. The myocardial mechanics of these patients showed a reduced strain in the areas of hypertrophy without involvement of the adjacent nonhypertrophied segments (Fig. 1B).

Age of the patients in the 5 cases ranged from 35 to 73 years; 4 patients were male. Dyspnea was the common symptom. Three patients had sleep apnea. Electrocardiograms of all patients revealed marked T-wave inversions in precordial leads, typical of apical HCM. Basal septal thickness ranged from 20 to 24 mm and apical thickness from 15 to 20 mm. The midventricular thickness in all of these patients was measured to be <12 mm in women and <13 mm in men. There were varying degrees of systolic anterior motion of mitral leaflets. Three patients had delayed gadolinium enhancement (DGE) on CMR involving the apex and basal septum. All patients received optimal medical treatment for symptoms attributable to left ventricular outflow tract obstruction. Three patients underwent alcohol septal ablation. Two patients received implantable cardioverter-defibrillators (ICDs) due to syncopal episodes and DGE; a third patient had sudden cardiac death prior to ICD implantation. Four patients underwent genetic testing, and no mutations were found.

The age of the 5 patients with HCM used for comparison ranged from 20 to 78 years; 2 were male. Three had basal septal hypertrophy, 1 had basal septal hypertrophy with some involvement of the midventricle, and 1 had localized apical hypertrophy. Ventricular wall thickness ranged from 19 to 22 mm, and mild left ventricular outflow tract obstruction was present in septal variants. Also included was a patient with genotype positive for a myosin heavy chain 7 gene mutation but phenotype negative, with normal global and regional longitudinal strain. One patient had a tropomyosin

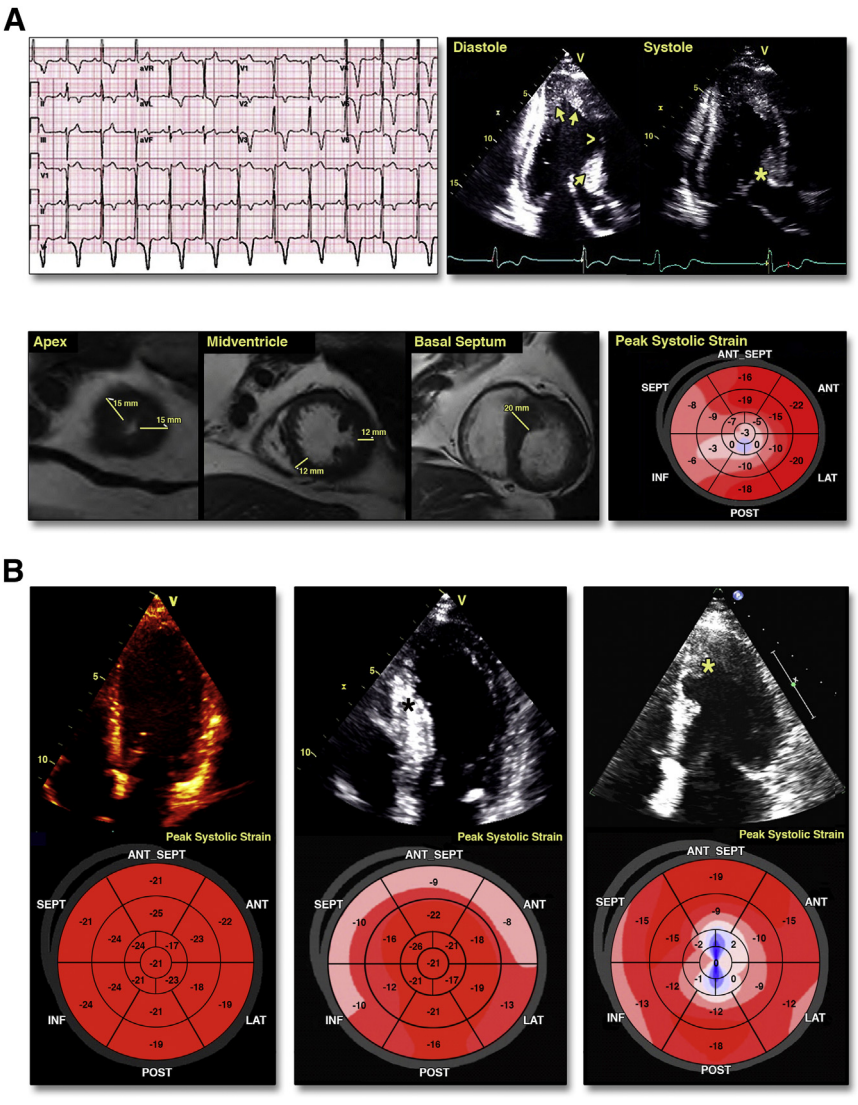

Figure 1. Multimodality Evaluation of Noncontiguous Hypertrophic Cardiomyopathy and Evaluation of Hypertrophic Cardiomyopathy Used for Comparison

(A, top left) Illustrative electrocardiogram demonstrates left ventricular hypertrophy and giant T-wave inversions in leads V3 to V6, typical of apical hypertrophic cardiomyopathy. **(A, top right)** Echocardiographic end-diastolic view **(left)** demonstrates marked apical and basal septal hypertrophy **(arrows)**. The intervening midventricular segments were spared of hypertrophy **(arrowhead)**. End-systolic view **(right)** demonstrates systolic anterior motion of the mitral leaflet **(asterisk)**. **(A, bottom left)** End-diastolic magnetic resonance images show marked circumferential hypertrophy of apex and basal anterior septum with normal midventricular segments. **(A, bottom right)** Illustrative speckle tracking echocardiographic polar plots demonstrate decreased global longitudinal systolic strain of −11%. Longitudinal strain was normal at anterolateral and inferolateral segments, but decreased regional strain was noted not only in the anterobasal septum and apex but also involved the intervening midventricular segments of normal thickness. This reflects that the myopathic process extended in a spiral manner from the basal septum toward the apex. Illustrative echocardiographic images of patients with hypertrophic cardiomyopathy (HCM) used for comparison with noncontiguous HCM cases. **(B, left)** Genotype-positive, phenotype-negative patient with normal global and regional longitudinal strain. **(B, middle)** Genotype-positive, phenotype-positive patient with HCM localized to basal septum with decreased regional longitudinal strain localized to the corresponding areas of basal septum. **(B, right)** Genotype-negative, phenotype-positive patient with HCM localized to the apex with decreased regional longitudinal strain localized to the corresponding areas of apex. Nonhypertrophied segments demonstrate normal longitudinal strain. ANT = anterior; ANT_SEPT = anteroseptal; INF = inferior; LAT = lateral; POST = posterior; SEPT = septal.

gene mutation, and another had a mutation involving the cardiac myosin-binding protein C gene. All patients received optimal medical treatment based on symptoms. One received ICD for nonsustained ventricular tachycardia and syncope.

Similar to the recently described spiral pattern of hypertrophy from the basal septum to the apex on CMR (3,4), our observations suggest that myocardial mechanics can also identify this continuum. In patients with noncontiguous HCM, speckle tracking

echocardiography may unveil myocardial dysfunction in the otherwise nonhypertrophied segments seen on conventional 2-dimensional echocardiography and CMR imaging. The major limitation of this study is the small number of patients; thus, these findings need to be further validated. Although we continue to try to solve the Rubik's Cube that is the left ventricle in normal and diseased states (5), especially with regard to HCM, further insights provided by myocardial mechanics in these patients could help guide our moves.

Anushree Agarwal, MD, Bijoy K. Khandheria, MD,* Timothy E. Paterick, MD, JD, Daniel Bloomgarden, MD, Rachel Loberg, ARNP, Michelle Bush, ARNP, A. Jamil Tajik, MD

*Aurora Cardiovascular Services, 2801 W. Kinnickinnic River Parkway, #840, Milwaukee, Wisconsin 53215. *E-mail: publishing22@aurora.org*

http://dx.doi.org/10.1016/j.jcmg.2013.04.016

REFERENCES

1. Maron MS, Maron BJ, Harrigan C, et al. Hypertrophic cardiomyopathy phenotype revisited after 50 years with cardiovascular magnetic resonance. J Am Coll Cardiol 2009;54:220–8.
2. Rickers C, Wilke NM, Jerosch-Herold M, et al. Utility of cardiac magnetic resonance imaging in the diagnosis of hypertrophic cardiomyopathy. Circulation 2005;112:855–61.
3. Florian A, Masci PG, De Buck S, et al. Geometric assessment of asymmetric septal hypertrophic cardiomyopathy by CMR. J Am Coll Cardiol Img 2012;5:702–11.
4. Reichek N. Seeing spirals. J Am Coll Cardiol Img 2012;5:712–4.
5. Sengupta PP, Narula J. LV segmentation and mechanics in HCM: twisting the Rubik's Cube into perfection! J Am Coll Cardiol Img 2012;5:765–8.

De-Novo Thrombus Formation and Latent Ligation Failure Following LAA Exclusion

Left atrial appendage (LAA) exclusion is becoming a popular alternative for patients with atrial fibrillation who are ineligible for long-term anticoagulation. The LAA exclusion system (Lariat Suture Delivery Device, SentreHEART Inc., Redwood City, California) was evaluated in a non-randomized single-center study with an immediate closure success rate (<1 mm of residual flow) of 95%, which was maintained up to 90 days as assessed by transesophageal echocardiography (TEE). The recent data has demonstrated safety and efficacy up to 1 year following the procedure with the success rate of up to 98% with no reported late device-associated thrombi (1,2). We report 3 cases of importance with respect to management of antiplatelet and anticoagulation therapy.

Patient #1. The first patient is a 63-year-old man with paroxysmal atrial fibrillation and prior splenic infarct who was ineligible for long-term anticoagulation because of underlying coagulopathy secondary to cryptogenic cirrhosis with a history of esophageal variceal bleed. Intraoperative TEE confirmed closure of the LAA with no evidence of residual leak immediately following the Lariat procedure (Fig. 1A). The patient received no post-operative antiplatelet or anticoagulant therapy. Routine follow-up TEE 3 months later showed that the LAA remained obliterated; however, there was a new mobile thrombus in the LAA remnant attached to the atrial wall (Fig. 1B). Despite his bleeding risk, the patient was started on warfarin and remained asymptomatic with no neurologic sequelae. Repeat TEE 2 months later showed complete resolution of thrombus.

Patient #2. The second patient is a 75-year-old woman with persistent atrial fibrillation and history of ischemic stroke who had extreme difficulty in maintaining a therapeutic international normalized ratio on warfarin. During the LAA exclusion procedure, it was difficult to obtain complete ostial closure of the LAA. Intraoperative imaging with angiography and TEE showed a small pouch remnant, but suggested most of the distal trabeculated appendage was closed (Fig. 1C). This patient also received no post-operative antiplatelet or anticoagulant therapy. Routine follow-up by TEE 3 months later revealed a thrombus in the LAA, which no longer appeared to be closed, suggesting latent ligation failure (Fig. 1D).

Patient #3. Finally, a 76-year-old man also with persistent atrial fibrillation was referred for the LAA exclusion procedure because of a history of intracerebral hemorrhage in addition to gastrointestinal bleed while on warfarin. Intraoperative TEE and angiography confirmed complete closure of the LAA with no residual leak (Fig. 1E). At discharge, the patient was maintained on aspirin and clopidogrel only. Follow-up TEE 3 months later demonstrated thrombus formation in the LAA, which was no longer ligated (Fig. 1F). Because of the presence of thrombus, aspirin and clopidogrel were discontinued, and the patient was started on warfarin.

Initially, the role of post-procedure antithrombotic therapy was largely unknown, although it was suggested the Lariat device would allow freedom from warfarin, especially immediately following the procedure. This is a contradistinction to another LAA closure device (Watchman, Boston Scientific, Natick, Massachusetts), which requires warfarin post-operatively for at least 45 days while the device endothelializes (3). Initially, the role of anticoagulation immediately following the Lariat procedure was unclear and a nonsystematic approach was applied. Recent data showing long-term results for thromboembolic event reduction are confounded by the high proportion of patients (61%) on warfarin at the time of last follow-up (approximately 1 year). Because this data can not confirm freedom from thrombus formation without anticoagulation, recent recommendations by Bartus et al. (2) now suggest that patients with a $CHADS_2$ (congestive heart failure; hypertension >140/90 mm Hg, or on hypertension medication; age ≥75 years; diabetes mellitus; and prior stroke, transient ischemic attack, or thromboembolism) score of 2 or higher who can tolerate anticoagulation continue warfarin.

As noted in this report, we present a case series of 3 patients who at 3-month follow-up TEE, had evidence of de novo thrombus formation: 1 adjacent to the ligated LAA; and 2 within the LAA that no longer appeared to be ligated. One patient received antiplatelet therapy; however, none were initiated on anticoagulant therapy immediately after the procedure. Based on